

# ANALYSIS AND PREVENTION OF PHOSPHORUS CONTAMINATION DURING ANTIMONY IMPLANTATION

Marián Kuruc<sup>\*</sup> — Ladislav Hulényi<sup>\*\*</sup>  
Rudolf Kinder<sup>\*\*</sup> — Andrej Vincze<sup>\*\*\*</sup>

The influence of different levels of phosphorus dose in antimony implantation on the depth of p-n junction for a buried layer structure is analysed. Samples implanted on implanters with different levels of phosphorus cross-contamination are characterized by methods like SIMS, spreading resistance analysis (SRP) and simulations by SUPREM software. Experimental determination of the contamination dose from the carrier concentration profiles  $N_c(x)$  measured by SRP and simulated  $N_{dt}(x)$  profiles by SUPREM is presented. The use of a sacrificial oxide layer is also discussed and analysed as a possibility for prevention of phosphorus contamination in antimony implantation.

**Keywords:** ion implantation, cross-contamination, antimony, spreading resistance, SIMS, doping profile

## 1 INTRODUCTION

Ion implantation presents an important step of the semiconductor manufacturing process. It allows changing the conduction properties of semiconductors by introducing small quantities of dopant atoms and creating doping profiles that cannot be achieved by standard diffusion processes. The depth of the doping profile can be controlled by adjusting the implantation energy. The dopant dose can be controlled by monitoring the ion current during implantation. Since the implantation process causes disruptions in the silicon lattice caused by ion collisions, subsequent thermal treatment is required to repair the damage and to activate implanted dopants. This can be done by standard furnace annealing or by rapid thermal annealing.

Doping of advanced integrated circuits requires a very high level of purity for the material that arrives at the wafer surface. Ion implantation is basically considered to be a clean process because the mass separator separates contaminant ions from the beam before they reach the target. However, there are still several sources of contamination near the end of the beam line that can cause contaminant ions to reach the target. One possible source of contamination are metal atoms knocked off from the chamber walls, wafer holders and clips, *etc* [1]. After many implantations the internal surface of the implanter can also become saturated with dopants and they can contaminate the beam. When these contaminant atoms reach the surface of the wafer, they can be recoil implanted by primary ions deeper into the substrate. Then, during subsequent thermal processing, they can influence the elec-

tric properties of semiconductors. The impact of dopant cross-contamination is strongly dependent on the device structure, doping levels and the combination of dopants involved [2]. For advanced integrated circuits the dose of dopant cross-contamination needs to be controlled to less than  $10^{12}\text{cm}^{-2}$  [3, 4].

In this article we present experiments to determine phosphorous cross-contamination during antimony implant. For our experiments we used buried layer structure because this is created by antimony implantation followed by a long diffusion process. We have prepared samples implanted on an implanter with different levels of phosphorus contamination and analysed them by SIMS (Secondary Ion Mass Spectroscopy), TOF SIMS (Time of Flight SIMS) and SRP (Spreading Resistance Profiling analysis). We also present results from SUPREM-IV simulations for different levels of phosphorus contamination and analyse the capability of a sacrificial oxide layer to prevent it.

## 2 EXPERIMENTAL DATA

Our experiments were made on p-type (Boron) wafers, with 150 mm diameter, thickness  $675\mu\text{m}$ , crystallographic orientation  $\langle 111 \rangle$  and resistivity 5 to  $15\Omega\text{cm}$ . To determine phosphorous contamination on our implanter we used a buried layer  $^{121}\text{Sb}$  implantation. Implantation energy was  $E = 40\text{keV}$  and dose of  $^{121}\text{Sb}$ ,  $N_D = 2.37 \times 10^{15}\text{cm}^{-2}$ . We have conducted one month monitoring of the level of phosphorus contamination on implanter EATON GDS (GDS1). Sample BLIMPL1 was implanted as first, then one week later we implanted

<sup>\*</sup> ON Semiconductor Slovakia, a.s., Vrbovská cesta 2617/102, 921 01 Piešťany, Slovakia, e-mail: marian.kuruc@onsemi.com

<sup>\*\*</sup> Slovak University of Technology, Faculty of Electrical Engineering and Information Technology, Department of Microelectronics, Ilkovičova 3, 812 19 Bratislava, Slovakia, e-mail: lhulenyi@elf.stuba.sk

<sup>\*\*\*</sup> International Laser Center, Ilkovičova 3, 812 19 Bratislava, Slovakia

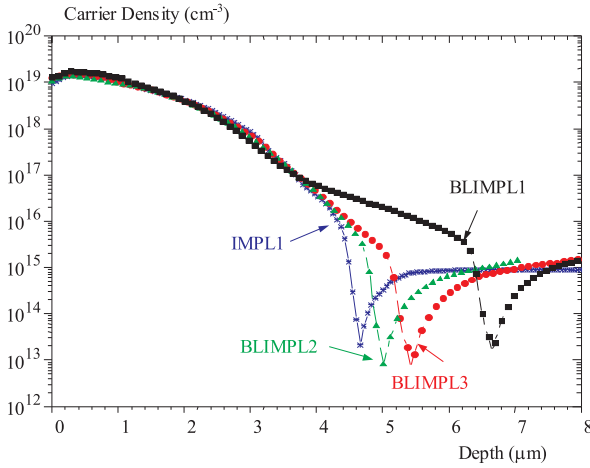


**Fig. 1.**  $N_c(x)$  profiles of sample IMPL1, BLIMPL1, BLIMPL2, BLIMPL3 measured by SRP.

samples BLIMPL2, two weeks later samples BLIMPL3 and BLIMPL4. Between implanting sample BLIMPL1 and the other samples the implanter was cleaned. We have also implanted one sample IMPL1 using another implanter EATON NV10-160. For samples BLIMP1, BLIMP2, BLIMP3 and IMPL1 the implantation process was followed by diffusion. The diffusion process consisted of 3 hour temperature rise to  $T = 1250^\circ\text{C}$  in nitrogen and oxygen atmosphere, followed by 180 min diffusion in nitrogen atmosphere, then 90 min temperature decreasing down to  $T = 975^\circ\text{C}$  and 110 min oxidization in wet  $\text{O}_2$ . After this process the oxide grown on samples was etched off.

On samples BLIMP1, BLIMP2, BLIMP3 and IMPL1 we measured the carrier concentration profiles  $N_c(x)$  using SSM2000 NanoSpreading Resistance Measurement system. The measured  $N_c(x)$  profiles are shown in Fig. 1.

As can be seen in Fig. 1,  $N_c(x)$  profiles measured by SRP show different depths of the p-n junction. The depth of p-n junction varies from  $4.7\ \mu\text{m}$  for sample Impl1 to  $6.6\ \mu\text{m}$  for sample BLIMPL1. This difference is caused by the presence of phosphorus in antimony implantation. Due to the long diffusion process the phosphorus diffuses deeper than antimony and causes a different depth of p-n junction. The diffusion coefficient for phosphorus is higher than for antimony. Both phosphorus and antimony diffuse by vacancy and also interstitial mechanisms. For phosphorus the dominant mechanism of diffusion is the interstitial mechanism. For antimony the vacancy mechanism dominates. The activation energies required for the diffusion of interstitial atoms are lower than those for diffusion of lattice atoms by vacancy mechanisms since no energy is required to form a vacancy [1]. This explains why phosphorus diffuses deeper into silicon than antimony.

To determine the dose of phosphorus in antimony implantation we analysed sample BLIMPL4 by SIMS. This analysis was performed using a Cameca Magnetic Sector SIMS instrument. Results of this analysis have shown that the dose of implanted antimony was for  $^{121}\text{Sb}$   $N_D =$

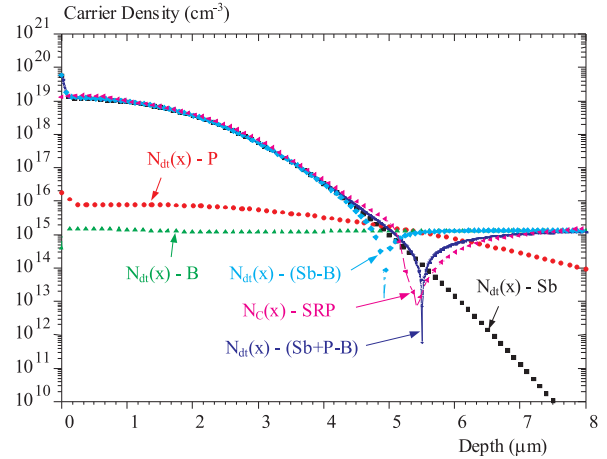


**Fig. 2.** Comparison of  $N_{dt}(x)$  profiles of Sb, P and B simulated by SUPREM-IV and  $N_c(x)$  profile measured by SRP on sample BLIMPL4.

$1.56 \times 10^{15}\text{cm}^{-2}$  and for  $^{123}\text{Sb}$   $N_D = 7.50 \times 10^{14}\text{cm}^{-2}$ . The total dose of Sb was then  $N_D = 2.31 \times 10^{15}\text{cm}^{-2}$ , which corresponds to the implanted dose  $N_D = 2.37 \times 10^{15}\text{cm}^{-2}$ . SIMS analysis also detected the dose of phosphorus  $N_D = 3.39 \times 10^{12}\text{cm}^{-2}$ .

To analyse the influence of this contamination dose on the final carrier concentration profile  $N_c(x)$  after diffusion, we have run simulations using SUPREM-IV software. For simulation of the antimony profile we used process parameters. To simulate implantation contamination we simulated implantation of phosphorus with a lower energy. We used the implantation energy  $E = 10\ \text{keV}$  and dose of phosphorus  $N_D = 3.39 \times 10^{12}\text{cm}^{-2}$ . This lower energy was used because SIMS analysis showed that phosphorus was implanted with much lower energy than antimony.

As can be seen in Fig. 2, the simulated doping profile  $N_{dt}(x)$  of (Sb-B) represents the doping profile without phosphorus contamination.  $N_{dt}(x)$  profile (Sb+P-B) represents contamination of phosphorus in antimony profile. The depth of this profile is  $0.6\ \mu\text{m}$  longer than the profile without phosphorus. The depth of  $N_{dt}(x)$  profile also corresponds to the depth determined from the carrier profile  $N_c(x)$  measured by SRP. From this experiment it can be seen that SUPREM simulation matches real carrier concentration profile measured by SRP on sample BLIMPL3. This sample was implanted together with sample BLIMPL4 and should have the same level of phosphorus contamination. As can be seen from these results, it is possible to estimate the dose of phosphorus in antimony implantation by comparing the simulated profile  $N_{dt}(x)$  and the profile  $N_c(x)$  measured by SRP (Fig. 2).

After we verified that the level of contamination could be determined from  $N_c(x)$  profiles measured by SRP and by simulations, we used SUPREM to simulate different doses of phosphorus in antimony profile. We simulated phosphorus doses from  $N_D(P) = 1 \times 10^{11}\text{cm}^{-2}$  to  $N_D(P) = 5 \times 10^{13}\text{cm}^{-2}$  and analysed the influence of

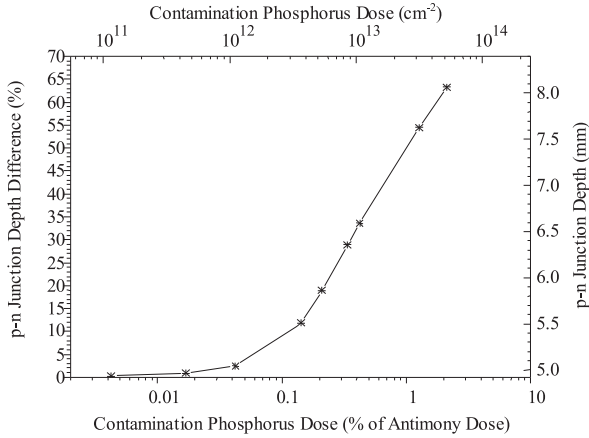


**Fig. 3.** Simulated dependence of p-n junction depth of a buried layer for different levels of phosphorus contamination during antimony implantation.

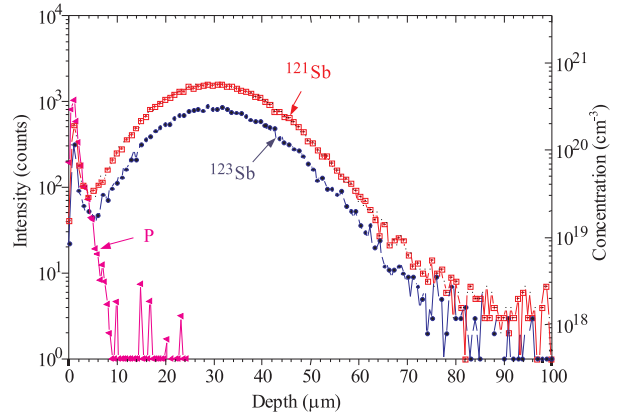


**Fig. 4.** TOF SIMS analysis of sample Impl5 (implantation without screen oxide).

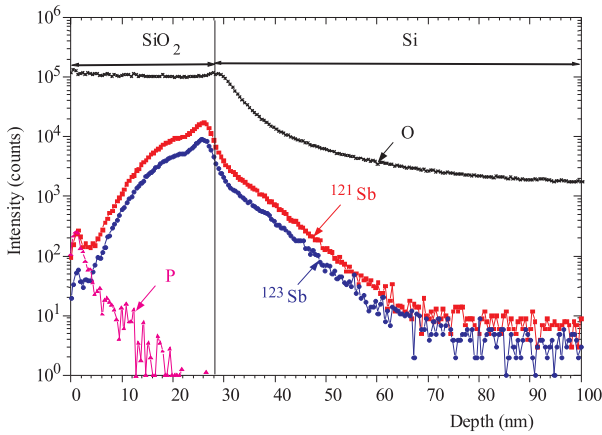


**Fig. 5.** TOF SIMS analysis of sample Impl6 (implantation with a 26 nm screen oxide).

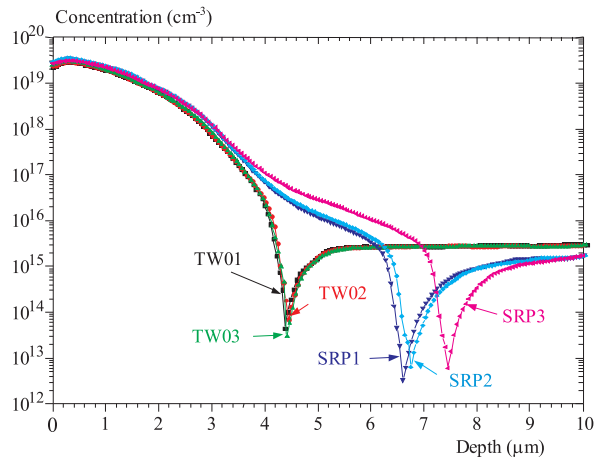


**Fig. 6.** Comparison of  $N_c(x)$  profiles of samples TW01, TW02, TW03, SRP1, SRP2, SRP3 measured by SRP.

this dose on the depth of p-n junction. Results of these simulations are shown in Fig. 3.

From Fig. 3 we can see that even a dose of phosphorus  $N_D(P) = 1 \times 10^{12} \text{cm}^{-2}$  causes a 2.5% shift in the p-n junction depth  $x_j$ . Phosphorus dose  $N_D(P) = 3 \times 10^{13} \text{cm}^{-2}$  in antimony implant causes a 54.5% shift in the depth of the p-n junction. Using the data from simulations we were able to determine the phosphorus contamination dose for samples BLIMPL1, BLIMPL2 and BLIMPL3. For sample BLIMPL1 the depth of p-n junction was  $x_j = 6.6 \mu\text{m}$ , which indicates the dose of phosphorus  $N_D(P) = 1.1 \times 10^{13} \text{cm}^{-2}$ . For sample BLIMPL2 the depth of p-n junction was  $x_j = 5 \mu\text{m}$ , which indicates the dose of phosphorus  $N_D(P) = 1 \times 10^{12} \text{cm}^{-2}$ . For sample BLIMPL3 the depth of p-n junction was  $x_j = 5.5 \mu\text{m}$  and corresponds the dose of phosphorus  $N_D(P) = 3.4 \times 10^{12} \text{cm}^{-2}$ .

After finding out that the level of contamination varies with time we have decided to test the possibility of using a sacrificial oxide layer (screen oxide) to prevent this contamination from getting into silicon. We have pre-

pared 2 samples. Both wafers were of the same type as those used in previous experiments. On sample SCTEST we have grown a 26 to 28 nm thick oxide layer. The other sample NOSCTEST was without oxide. Both samples were implanted  $^{121}\text{Sb}$  with  $E = 40 \text{keV}$  and dose  $N_D = 2.37 \times 10^{15} \text{cm}^{-2}$ . Samples were then analysed by TOF SIMS. The time of flight based SIMS instrument (Ion-TOF, SIMS IV) with high energy  $\text{Au}^+$  primary source was employed for the analysis of the implanted Si structure. For depth profiling of the structure, the high energy pulsed primary gun is combined with low energy sputter guns ( $\text{Cs}^+$ ,  $\text{O}_2^+$ ) because of their low erosion rate. The sputtering ion beam is scanned over an area of  $300 \times 300 \mu\text{m}$  while the primary beam is scanned within a  $70 \times 70 \mu\text{m}$  area in the centre of the sputtered area. TOF detection is performed by a single particle counting using microchannel plate detector with parallel mass detection in the range up to 8.000 amu (atomic mass units).

Results of TOF SIMS analysis are shown in Fig. 4 (sample NOSCTEST without oxide) and Fig. 5 (sample SCTEST with oxide layer). As can be seen in Fig. 4, phosphorus is concentrated mostly near the surface and

the concentration drops down below the detection limit of TOF SIMS at approximately 20 nm. When we look at Fig. 5, we can see that the contamination dose of phosphorus is trapped in the oxide layer. However, also part of antimony dose remains in the oxide and therefore will be removed together with the oxide layer. This is the reason why it is necessary to compensate for this loss of dose by increasing the implantation energy and dose. In our experiments we have found that increasing the implantation energy to 60 keV and  $^{121}\text{Sb}$  dose to  $N_D = 2.68 \times 10^{15} \text{cm}^{-2}$  compensates for the dose loss in the oxide.

To monitor the effectiveness of the sacrificial oxide layer in prevention of phosphorus contamination we have prepared samples SRP1, SRP2, SRP3 and TW01, TW02, TW03. On samples TW01, TW02, TW03 we grew a 26 to 28 nm thick oxide layer and samples SRP1, SRP2, SRP3 were without oxide. Samples SRP1, SRP2, SRP3 were used to monitor the level of phosphorus contamination in our implanter. Samples TW01, TW02, TW03 were to verify the ability of the oxide layer to prevent phosphorus contamination. All samples were implanted with  $^{121}\text{Sb}$  dose  $N_D = 2.68 \times 10^{15} \text{cm}^{-2}$  and implantation energy  $E = 60$  keV. Samples were divided into 3 groups. Samples SRP1 and TW01 were implanted together on one day. Samples SRP2 and TW02 were implanted on day 3 and samples SRP3 and TW03 were implanted together on day 5. The following diffusion process for all the samples was the same as for samples BLIMP1, BLIMP2, BLIMP3 and IMPL1. All samples were processed together to reduce differences during diffusion. The oxide was then etched off the samples. The  $N_c(x)$  profiles were then measured for all the samples by SRP. The results of this analysis are shown in Fig. 6.

As can be seen in Fig. 6, the samples with screen oxide (TW01, TW02, TW03) have the same  $N_c(x)$  profiles and these profiles show no contamination by phosphorus. The samples implanted without the oxide layer, however, show different levels of phosphorus contamination. Sample SRP3 shows the highest level of phosphorus contamination. When we use Fig. 3 to estimate the dose of phosphorus for sample SRP3, then it is approximately  $N_D = 2.8 \times 10^{13} \text{cm}^{-2}$ . However, the sample TW03 implanted together with this sample still shows no contamination. This confirms that the oxide layer with a thickness of 26 nm is able to prevent phosphorus contamination during antimony implantation.

There are also other possibilities to prevent this contamination like dedication of the implanter only for antimony implantation but this is a very expensive and ineffective solution. Also frequent cleaning of the implanter helps to reduce the phosphorus contamination but it cannot prevent it totally. The use of the sacrificial oxide layer seems to be the best solution and also has other advantages. This oxide also prevents contamination with metal atoms and reduces possible channelling effects.

### 3 CONCLUSION

We have presented methods that can be used to determine phosphorus contamination in antimony implant. We presented data from SIMS and TOF SIMS analysis, spreading resistance measurements, and simulations by SUPREM-IV. We have used SUPREM-IV to simulate the implantation contamination process. Good agreement between  $N_{dt}(x)$  profile from SUPREM-IV simulation and SRP data has been found (Fig. 2). Spreading resistance data combined with simulations can be used to determine the dose of implanted phosphorus after diffusion. We simulated different levels of phosphorus dose in antimony implant ( $N_D(P) = 1 \times 10^{11} \text{cm}^{-2}$  to  $5 \times 10^{13} \text{cm}^{-2}$ ) and its influence on  $N_d(x)$  profile and the depth of p-n junction  $x_j$  (Fig. 3) (shift of p-n junction  $\Delta x = 0.24\%$  to  $63.3\%$ ). From TOF SIMS analysis (Fig. 4) we have determined that the contamination dose of phosphorus is mostly concentrated near the silicon surface. From this we can assume that phosphorus is implanted with much lower energy than antimony. We have then analysed the possibility of using a 26 nm thick sacrificial oxide layer to prevent phosphorus from getting into silicon (Fig. 5). During implantation, phosphorus is trapped in the oxide layer and removed by etching. However, also part of the antimony dose is removed and it is necessary to adjust the implantation energy and the dose to compensate for this loss. We have also verified the functionality of this oxide layer for different levels of phosphorus contamination (Fig. 6) and determined that it is able to prevent the contamination even for high doses of phosphorus  $N_D = 2.8 \times 10^{13} \text{cm}^{-2}$ .

### Acknowledgements

This work was supported by VEGA grants 1/0152/03, 1/0130/03, 1/0154/03, and project APVT-20-013902.

### REFERENCES

- [1] SZE *et al*: VLSI Technology (Second Edition), McGraw-Hill International editions, 1988.
- [2] ZIEGLER, J. F.: Ion Implantation, Science and Technology, 2000 Edition, IIT Press, 2000, pp. 588–627.
- [3] LARSON, L. A.—CURRENT, M. I.—HEALY, C.: Enhanced Diffusion Effects and Dopant Cross-Contamination in Ion Implanted Surfaces, in Semiconductor Silicon 1986, Electrochemical Soc. Proc. 86-4 (1986) 667.
- [4] CURRENT, M. I.—LARSON, L. A.: Ultra-Pure Processing: A Key Challenge for Ion Implantation for Fabrication of ULSI Devices, Ion Beam Processing of Advanced Electronics Materials, Material Research Soc. Proc. 147 (1989) 365.

Received 6 May 2005

Marián Kuruc (Ing), Ladislav Hulényi (Doc, Ing, PhD), Rudolf Kinder (Doc, Ing, PhD), Andrej Vincze (Ing). Biographies not supplied.